

Photon induced processes from semi-central to ultraperipheral heavy-ion collisions

Wolfgang Schäfer^{a,*}

^a*Institute of Nuclear Physics, Polish Academy of Sciences
ul. Radzikowskiego 152, PL-31-342 Kraków, Poland*

E-mail: wolfgang.schafer@ifj.edu.pl

Ultrarelativistic heavy ions are accompanied by a large flux of quasi-real Weizsäcker-Williams photons. This opens a broad range of research possibilities, as the Weizsäcker-Williams photons can be used to study photon-photon fusion reactions as well as photonuclear reactions in a wide range of energies.

Of special interest here are diffractive photoproduction reactions, which appear in two major classes: the coherent diffraction in which the target nucleus stays intact and the incoherent (or quasielastic) diffraction in which the nucleus breaks up, but no additional particles are produced in the nuclear fragmentation region.

We will discuss the coherent diffractive photoproduction of heavy vector mesons J/ψ . Good agreement with available experimental data by the ALICE and LHCb collaborations can be obtained within a color-dipole approach. Here additional nuclear shadowing from the $c\bar{c}g$ -Fock state is needed to obtain agreement with data.

Very recently, the role of Weizsäcker-Williams photons in peripheral, inelastic, heavy ion collisions has come under scrutiny. Recent measurements of dilepton production of the STAR collaboration in $\sqrt{s_{NN}}=200$ GeV Au-Au collisions indicate an excess at small pair p_T most notably in peripheral collisions. We show, that it can be that has attributed to the initial photon fusion which is most significant at small pair transverse momenta. The centrality dependence of the pair transverse momentum distribution is calculated in a novel factorization approach involving Wigner distributions of photons.

*XV International Workshop on Hadron Physics (XV Hadron Physics) 13 -17 September 2021
Online, hosted by Instituto Tecnológico de Aeronáutica, São José dos Campos, Brazil*

*Speaker

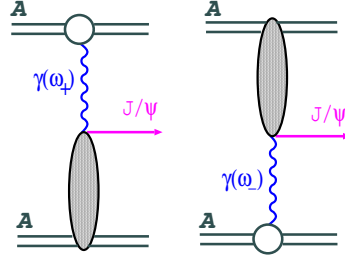


Figure 1: Feynman diagrams for the exclusive photoproduction of J/ψ in a nucleus-nucleus collision.

1. Introduction

Electrically charged particles in ultrarelativistic motion are the source of an electromagnetic field, which invariants fulfill $\vec{E}^2 - \vec{B}^2 \sim 0$, $\vec{E} \cdot \vec{B} \sim 0$. The field carries energy and momentum, has a nonvanishing Poynting vector, and can be interpreted as a flux of quasi-real Weizsäcker-Williams photons. In practical terms, the method of quasireal photons has many applications to the ultraperipheral collisions of heavy ions of charge Ze , see for example the reviews [1–3]. The Weizsäcker-Williams photons are the prototypical partons, and one may ask whether these partons, which are enhanced by the large factor Z^2 , also play a role in central or semicentral, and hence inelastic, nuclear collisions. Early considerations of such processes can be found, e.g. in [4].

Here give an overview of a few photon induced processes from ultraperipheral to semi-central heavy ion collisions. Firstly, the exclusive diffractive photoproduction of J/ψ mesons, and secondly the production of lepton pairs in semicentral collisions. For more background and references, see Ref. [5].

2. Exclusive diffractive photoproduction of J/ψ

The exclusive photoproduction of vector mesons in ultrarelativistic heavy ion collisions was pioneered by Klein and Nystrand [6] and Gonçalves and Machado [7]. Here one of either ions can play the role of the source of the photon flux, while the photoproduction reaction $\gamma A \rightarrow J/\psi A$ proceeds on the other ion. This means, that in general there is an interference between the two diagrams in Fig. 1. This interference would introduce a correlation $\propto \mathbf{p}_1 \cdot \mathbf{p}_2$ between the transverse momenta of outgoing ions [8], which would not contribute to the rapidity distribution of mesons. We thus end up with two contributions to the cross sections added incoherently:

$$\frac{d\sigma(AA \rightarrow AAJ/\psi; \sqrt{s_{NN}})}{dy} = n(\omega_+) \sigma(\gamma A \rightarrow J/\psi A; W_+) + n(\omega_-) \sigma(\gamma A \rightarrow J/\psi A; W_-).$$

Here the photon energies are given by $\omega_{\pm} = m_{J/\psi} \exp[\pm y]/2$, and the corresponding cms-energies for the $\gamma A \rightarrow J/\psi A$ subprocesses are $W_{\pm} = 2\sqrt{s_{NN}}\omega_{\pm}$. As an example, at midrapidity, the γA -cm energy W is $W = 92.5$ GeV for $\sqrt{s_{NN}} = 2.76$ TeV and $W = 125$ GeV for $\sqrt{s_{NN}} = 5$ TeV. The recent measurements [16–19] of exclusive production of J/ψ mesons in ultraperipheral heavy-ion collisions at the LHC thus have given us access to the interaction of small color dipoles with cold nuclear matter, partially in an energy range not studied before.

To this end, recall that in the limit of large photon energy ω in the rest frame of the nucleus, the coherence length $l_c = 2\omega/M_{J/\psi}^2$ becomes much larger than the size of the nucleus $l_c \gg R_A$ [9, 10]. It is then convenient, to describe the photoproduction of the J/ψ as a splitting of the photon into a $c\bar{c}$ pair far upstream the target, and an interaction of a color dipole of size \mathbf{r} formed by quark and antiquark. After the interaction with the target, the scattered $c\bar{c}$ pair evolves into the outgoing final state vector meson. The dominantly imaginary forward amplitude for this process then takes the form

$$\begin{aligned} \mathcal{A}(\gamma A \rightarrow J/\psi A; W, \mathbf{q} = 0) &= 2i \int d^2\mathbf{b} \langle J/\psi | \Gamma_A(x, \mathbf{b}, \mathbf{r}) | \gamma \rangle \\ &= 2i \int_0^1 dz \int d^2\mathbf{r} \Psi_{J/\psi}^*(z, \mathbf{r}) \Psi_\gamma(z, \mathbf{r}) \int d^2\mathbf{b} \Gamma_A(x, \mathbf{b}, \mathbf{r}). \end{aligned} \quad (1)$$

Here W is the γA per-nucleon cm-energy, and $x = M_{J/\psi}^2/W^2$. Here z is the lightcone momentum fraction of the photon momentum carried by the quark. The $c\bar{c}$ -Fock state light-front wave functions of photon and J/ψ are denoted by Ψ_γ and $\Psi_{J/\psi}$ respectively. The quark/antiquark helicities are conserved in the interaction with the target and are not shown in our notation.

In our recent work [11–13] we used a nuclear dipole cross section which was based on its free-nucleon counterpart obtained through fits to precise HERA data [14, 15].

The approach used in Refs.[11, 12], was based on dipole-nucleus amplitudes obtained from applying Glauber-theory to color dipoles understood as a set of eigenstates of the scattering.

Under this assumption, plus the standard lore of treating the nucleus as a dilute system of nucleons, the dipole-nucleus amplitude in impact parameter space is immediately obtained as:

$$\Gamma_A(x, \mathbf{b}, \mathbf{r}) = 1 - S_A(x, \mathbf{b}, \mathbf{r}), \quad \text{with } S_A(x, \mathbf{b}, \mathbf{r}) = \exp \left[-\frac{1}{2} \sigma(x, \mathbf{r}) T_A(\mathbf{b}) \right]. \quad (2)$$

Here the optical thickness of the nucleus is given by $T_A(\mathbf{b}) = \int_{-\infty}^{\infty} dz n_A(\sqrt{\mathbf{b}^2 + z^2})$, with the nuclear matter density $n_A(R)$ being normalized as $\int d^3\vec{R} n_A(R) = A$. The result Eq.2 corresponds to a summation of diagrams of the type shown in Fig. 2a. It takes into account the multiple scattering of the $c\bar{c}$ -dipole on the constituent protons and neutrons of the nucleus.

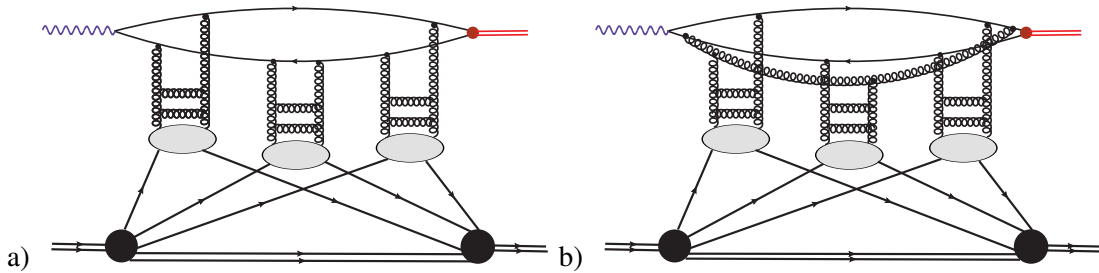


Figure 2: Coherent photoproduction of a vector meson in which the nucleus stays in its ground state.

With increasing energy, the coherency condition $l_c \gg R_A$ will be satisfied not only by the $c\bar{c}$ -state, but also by higher $c\bar{c}g$ states shown in in Fig. 2b. The effect of these higher Fock-states amounts to inelastic shadowing corrections induced by high-mass diffractive states.

One now extends the Fock-state expansion of the photon as

$$|\gamma\rangle = \sqrt{Z_g} \Psi_{c\bar{c}} |c\bar{c}\rangle + \Psi_{c\bar{c}g} |c\bar{c}g\rangle + \dots \quad (3)$$

Here $\Psi_{c\bar{c}}, \Psi_{c\bar{c}g}$ are the light-front wavefunctions (WFs) of the two- and three-body Fock states respectively. The factor $\sqrt{Z_g}$ is a (formally infinite) wave function renormalization. For gluons which carry a small light-cone momentum fraction $z_g \ll 1$, the three-body WF takes a factorized form, $\Psi_{c\bar{c}g} = \Psi_{c\bar{c}} (\Psi_{cg} - \Psi_{\bar{c}g})$.

As for the $c\bar{c}$ -dipole, also for higher Fock states, the impact parameters and helicities of partons are conserved. We denote the c - g and \bar{c} - g transverse distances by ρ_1 and ρ_2 , respectively, and the $c\bar{c}$ separation by $\mathbf{r} = \rho_1 - \rho_2$. Then, following Ref.[22], the dipole cross section for the three-body system is

$$\sigma_{q\bar{q}g}(x, \rho_1, \rho_2, \mathbf{r}) = \frac{C_A}{2C_F} \left(\sigma(x, \rho_1) + \sigma(x, \rho_2) - \sigma(x, \mathbf{r}) \right) + \sigma(x, \mathbf{r}), \quad (4)$$

where $C_A = N_c$ and $C_F = (N_c^2 - 1)/(2N_c)$ are the standard color factors.

The nuclear S -matrix for the $c\bar{c}g$ -state would now be obtained from applying the Glauber-form to the cross section Eq.(4). In a large- N_c approximation, the three-body S -matrix factorizes as

$$S_{q\bar{q}g,A}(x, \rho_1, \rho_2, \mathbf{b}) = S_A(x, \rho_1, \mathbf{b} + \frac{\rho_2}{2}) S_A(x, \rho_2, \mathbf{b} + \frac{\rho_1}{2}) \quad (5)$$

Taking due care of the virtual correction to the two-body Fock state, after integrating over degrees of freedom of the gluon, we obtain the full dipole-nucleus amplitude as:

$$\Gamma_A(x, \mathbf{r}, \mathbf{b}) = \Gamma_A(x_A, \mathbf{r}, \mathbf{b}) + \log\left(\frac{x_A}{x}\right) \Delta\Gamma_A(x_A, \mathbf{r}, \mathbf{b}), \quad (6)$$

with the correction to the dipole-amplitude from the $c\bar{c}g$ state:

$$\begin{aligned} \Delta\Gamma_A(x_A, \mathbf{r}, \mathbf{b}) = & \int d^2\rho_1 |\psi(\rho_1) - \psi(\rho_2)|^2 \left\{ \Gamma_A(x_A, \rho_1, \mathbf{b} + \frac{\rho_2}{2}) + \Gamma_A(x_A, \rho_2, \mathbf{b} + \frac{\rho_1}{2}) \right. \\ & \left. - \Gamma_A(x_A, \mathbf{r}, \mathbf{b}) - \Gamma_A(x_A, \rho_1, \mathbf{b} + \frac{\rho_2}{2}) \Gamma_A(x_A, \rho_2, \mathbf{b} + \frac{\rho_1}{2}) \right\}, \quad (7) \end{aligned}$$

Here the logarithm in Eq.(6) comes from the integration over the longitudinal phase-space of the gluon, where the WF of the gluon with $z_g \ll 1$ leads to the dz_g/z_g integration. There remains a dependence on transverse separation of the gluon from quark/antiquark, encoded in the radial WF:

$$\psi(\rho) = \frac{\sqrt{C_F\alpha_s}}{\pi} \frac{\rho}{\rho R_c} K_1\left(\frac{\rho}{R_c}\right) \quad (8)$$

In Eq.(7) the integration extend over all dipole sizes, including the infrared domain of large dipoles, where perturbation theory does not apply. Here, we follow [23, 24]. by introducing the minimal regularization of pQCD in terms of the finite propagation radius $R_c \sim 0.2 \div 0.3$ fm accompanied by a corresponding freezing of α_s in the infrared.

In our numerical calculations we use the same light-front wave function as used in [12], and the dipole cross section obtained in [15]. We refer the reader to these references to details which cannot be repeated here.

In Fig.3a) we compare to data of ALICE and CMS at $\sqrt{s_{NN}} = 2.76$ TeV, while Fig.3b) we show the comparison with data of LHCb and ALICE at $\sqrt{s_{NN}} = 5.02$ TeV, .

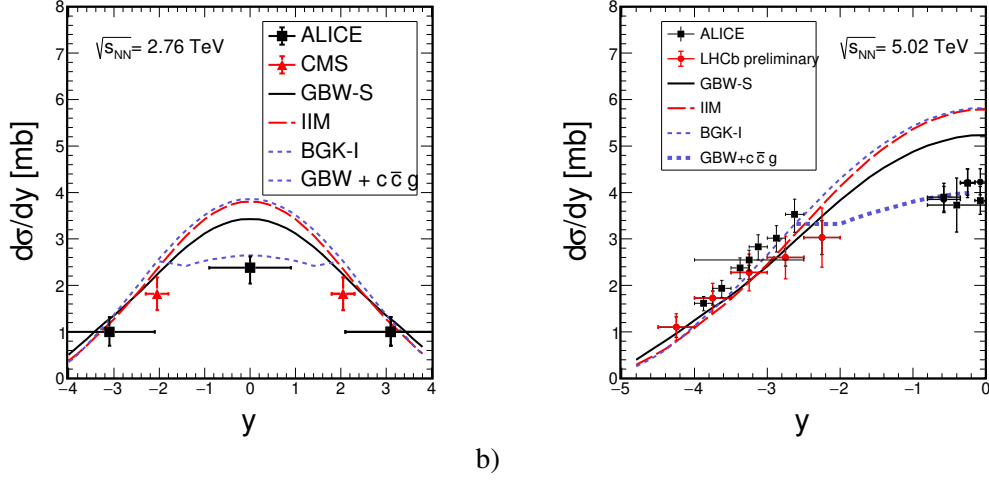


Figure 3: Rapidity dependent cross section from the coherent photoproduction of J/ψ in lead-lead collisions for two different energies. The thick dashed curve contains the $c\bar{c}g$ -state with $R_c = 0.215$ fm.

3. Centrality dependence of dilepton production via the $\gamma\gamma$ fusion

Recently, the STAR collaboration at RHIC has measured dilepton pairs in three centrality classes down to very small P_T of the pair and observes a large enhancement for $P_T < 150$ MeV. Dileptons are a “classic” probe of the strongly interacting matter/ quark gluon plasma (QGP) produced in the collision, see for example Ref. [25, 26] for reviews. A part of the spectrum carries information on the medium modifications of light vector mesons, and there is also a contribution of thermal dileptons.

Now, a natural production mechanism of dilepton pairs with very small pair transverse momentum is the $\gamma\gamma$ -fusion mode. So indeed it is natural to ask if the Weizsäcker-Williams photons play a role also in inelastic collisions. Here we should think of the strongly interacting nuclei to give rise to an “underlying event”, in which even a quark-gluon plasma can be formed.

In Ref. [27], we investigated the interplay between different dilepton production mechanisms. We included the thermal dilepton production from a near-equilibrated medium following the approach of [28]. The calculation of the coherent photon contribution is set up in impact parameter space. The relevant cross section is obtained from a convolution of the standard Weizsäcker-Williams fluxes, which as an input need only the nuclear charge form factor:

$$\frac{d\sigma_{ll}}{d\xi d^2\mathbf{b}} = \int d^2\mathbf{b}_1 d^2\mathbf{b}_2 \delta^{(2)}(\mathbf{b} - \mathbf{b}_1 - \mathbf{b}_2) N(\omega_1, b_1) N(\omega_2, b_2) \frac{d\sigma(\gamma\gamma \rightarrow l^+l^-; \hat{s})}{d(-\hat{t})}. \quad (9)$$

Here the phase space element is $d\xi = dy_+ dy_- dp_t^2$ with y_{\pm} , p_t and m_l the single-lepton rapidities, transverse momentum and mass, respectively. The photon energies $\omega_{1,2}$ are fixed by the lepton momenta. The yield in a given centrality class C is given by

$$\frac{dN_{ll}[C]}{dM} = \frac{1}{f_C \cdot \sigma_{AA}^{\text{in}}} \int_{b_{\text{min}}}^{b_{\text{max}}} db \int d\xi \delta(M - 2\sqrt{\omega_1\omega_2}) \left. \frac{d\sigma_{ll}}{d\xi db} \right|_{\text{cuts}}, \quad (10)$$

where the relevant impact parameter ranges can be obtained by a simple optical limit Glauber calculation, and f_C is the fraction of inelastic events in the centrality bin C . In Fig. 4 we show our results for the invariant mass distribution of dileptons in three different centrality classes and compare them to the data by the STAR collaboration. We observe that in the most peripheral bin, the photon-induced dileptons almost exhaust the cross section. They dominate also in the 40-60% centrality range, whereas for the most central bin, thermal dileptons and hadronic cocktail contribute in similar amounts. In Ref. [27], we also studied the evolution of the interplay of the different mechanisms with energy. We have shown there, that thermal emission rises logarithmically with energy, while the $\gamma\gamma$ process is strongly energy dependent for $\sqrt{s_{NN}} < 100$ GeV and levels off roughly above RHIC energy.

In Fig. 5 we show the pair transverse momentum distributions for RHIC and LHC energies. We compare them to STAR data and preliminary data from ALICE. Our calculation was performed in two ways, firstly as a convolution of the transverse momentum-dependent photon fluxes:

$$\frac{dN(\omega, \mathbf{q})}{d^2\mathbf{q}} \propto |\mathbf{E}(\omega, \mathbf{q})|^2, \text{ with } \mathbf{E}(\omega, \mathbf{q}) \propto \frac{\mathbf{q}F_{\text{ch}}(\mathbf{q}^2 + \omega^2/\gamma^2)}{\mathbf{q}^2 + \frac{\omega^2}{\gamma^2}}. \quad (11)$$

The second method now incorporates the correlation between photon transverse momenta and the impact parameter of the collision. For a simultaneous description in momentum and configuration space a formulation based on Wigner-functions is appropriate [29].¹

More precisely, the relevant ingredient for the factorization formula is a Wigner transform of a polarization density matrix of Weizsäcker–Williams photons:

$$N_{ij}(\omega, \mathbf{b}, \mathbf{q}) = \int \frac{d^2\mathbf{Q}}{(2\pi)^2} \exp[-i\mathbf{b}\mathbf{Q}] E_i\left(\omega, \mathbf{q} + \frac{\mathbf{Q}}{2}\right) E_j^*\left(\omega, \mathbf{q} - \frac{\mathbf{Q}}{2}\right). \quad (12)$$

Here i, j are cartesian polarizations of photons. The cross section can be cast into a form which involves cross sections for photons in channels of angular momentum projection $J_z = 0, \pm 2$ and even or odd parity:

$$\begin{aligned} \frac{d\sigma}{d^2\mathbf{b}d^2\mathbf{P}} &= \int \frac{d^2\mathbf{Q}}{(2\pi)^2} \exp[-i\mathbf{b}\mathbf{Q}] \int \frac{d\omega_1}{\omega_1} \frac{d\omega_2}{\omega_2} \int \frac{d^2\mathbf{q}_1}{\pi} \frac{d^2\mathbf{q}_2}{\pi} \delta^{(2)}(\mathbf{P} - \mathbf{q}_1 - \mathbf{q}_2) \\ &\times E_i\left(\omega_1, \mathbf{q}_1 + \frac{\mathbf{Q}}{2}\right) E_j^*\left(\omega_1, \mathbf{q}_1 - \frac{\mathbf{Q}}{2}\right) E_k\left(\omega_2, \mathbf{q}_2 - \frac{\mathbf{Q}}{2}\right) E_l^*\left(\omega_2, \mathbf{q}_2 + \frac{\mathbf{Q}}{2}\right) \\ &\times \frac{1}{2\hat{s}} \left\{ \delta_{ik}\delta_{jl} \sum_{\lambda\bar{\lambda}} \left| M_{\lambda\bar{\lambda}}^{(0,+)} \right|^2 + \epsilon_{ik}\epsilon_{jl} \sum_{\lambda\bar{\lambda}} \left| M_{\lambda\bar{\lambda}}^{(0,-)} \right|^2 \right. \\ &\left. + P_{ik}^{\parallel} P_{jl}^{\parallel} \sum_{\lambda\bar{\lambda}} \left| M_{\lambda\bar{\lambda}}^{(2,-)} \right|^2 + P_{ik}^{\perp} P_{jl}^{\perp} \sum_{\lambda\bar{\lambda}} \left| M_{\lambda\bar{\lambda}}^{(2,+)} \right|^2 \right\} d\Phi(l^+l^-). \end{aligned} \quad (13)$$

with $\delta_{ik} = \hat{x}_i\hat{x}_k + \hat{y}_i\hat{y}_k$, $\epsilon_{ik} = \hat{x}_i\hat{y}_k - \hat{y}_i\hat{x}_k$, $P_{ik}^{\parallel} = \hat{x}_i\hat{x}_k - \hat{y}_i\hat{y}_k$, $P_{ik}^{\perp} = \hat{x}_i\hat{y}_k + \hat{y}_i\hat{x}_k$.

From Fig. 5, we see that the Wigner function approach agrees very well with data, while the naive photoproduction peak at slightly lower P_T than data. With increasing cm-energy (right

¹An approach to dilepton production based on Wigner functions has recently been proposed in [30], for a recent review with more references, see [31]

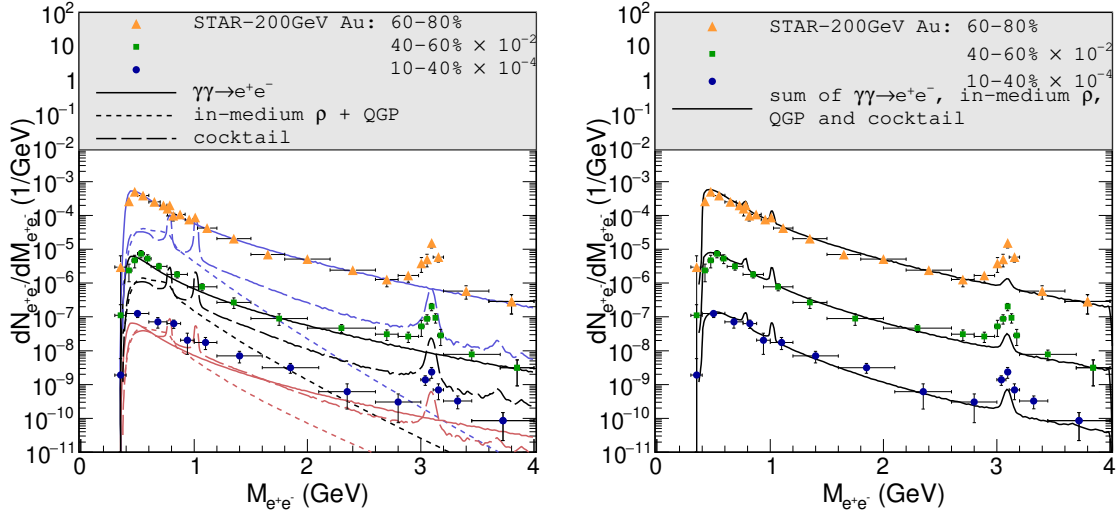


Figure 4: Left panel: Dielectron invariant-mass spectra for pair- $P_T < 0.15$ GeV in Au+Au($\sqrt{s_{NN}}=200$ GeV) collisions for 3 centrality classes including experimental acceptance cuts ($p_t > 0.2$ GeV, $|\eta_e| < 1$ and $|y_{e^+e^-}| < 1$) for $\gamma\gamma$ fusion (solid lines), thermal radiation (dotted lines) and the hadronic cocktail (dashed lines); right panel: comparison of the total sum (solid lines) to STAR data.

panel), the peak would run away towards smaller and smaller P_T , because ω/γ in Eq. 11 decreases with increasing boost parameter γ . The Wigner function approach completely solves this problem.

The dilepton system carries a finite total P_T , therefore dileptons are not back-to-back in the transverse plane. This is quantified by the acoplanarity: $\alpha = 1 - \frac{\Delta\phi}{\pi}$, or azimuthal decorrelation of electrons. We stress, that the Wigner-function approach has no free parameters, only the known e.m. form factors/charge distributions of nuclei enter the calculation. Main features of the preliminary ATLAS data are very well described by the Wigner function approach, see Fig. 6. There is perhaps some room for additional decorrelation effects (multiphoton exchanges, bremsstrahlung ...) at larger α .

4. Summary

We have demonstrated, that the ultraperipheral exclusive diffractive J/ψ production in the forward rapidity region is well described by Glauber-Gribov rescattering of $c\bar{c}$ -dipoles, with a dipole cross section fixed by precise HERA dat. At midrapidity however additional suppression is needed. A reasonable description is obtained after inclusion of $c\bar{c}g$ state, with a rather small gluon propagation radius $R_c \sim 0.2$ fm. The additional shadowing corresponds to a (moderate) shadowing of the nuclear glue. As an example for the role of Weizsäcker-Williams photons in (semi-)central nuclear collisions, we have studied low- P_T dilepton production in ultrarelativistic heavy-ion collisions, by a systematic comparisons of thermal radiation and photon-photon fusion within the coherent fields of the incoming nuclei. A comparison to recent STAR data gives a good description of low- P_T dilepton data in Au-Au($\sqrt{s_{NN}}=200$ GeV) collisions in three centrality classes, for invariant masses from threshold to ~ 4 GeV. The coherent emission is dominant for

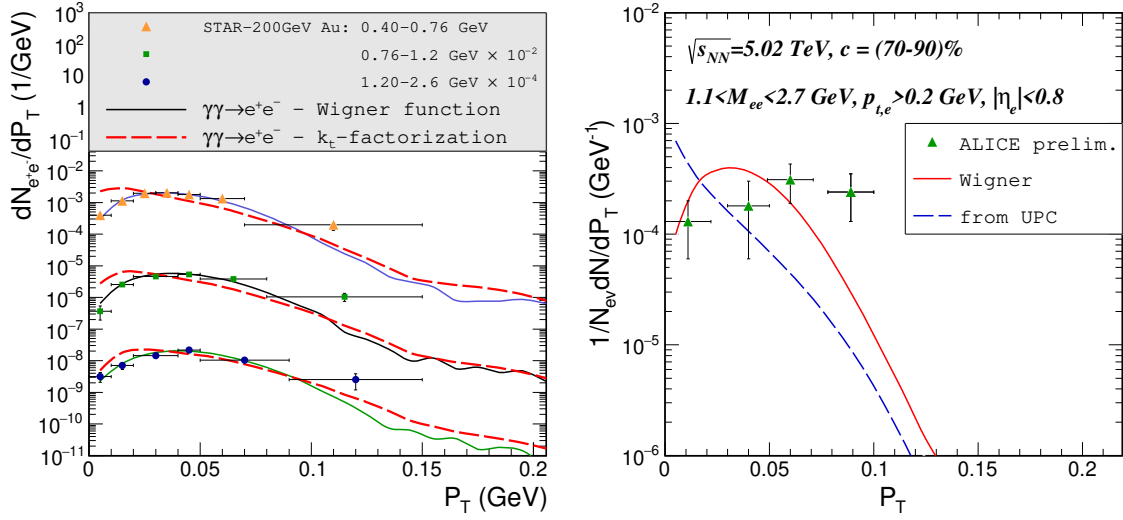


Figure 5: P_T -pair spectrum of dielectrons, left: ($\sqrt{s_{NN}}=200$ GeV) for centralities 60 - 80 %, right: for 70-90% centrality Pb + Pb collisions at ($\sqrt{s_{NN}}=5020$ GeV).

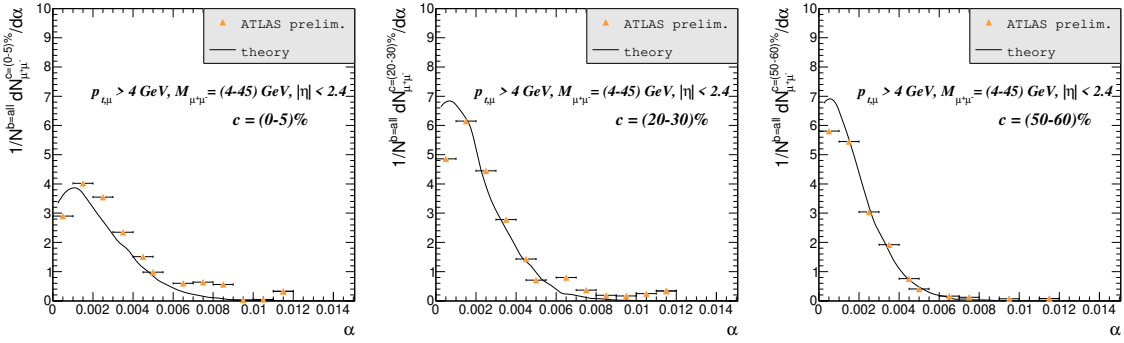


Figure 6: Acoplanarity distributions (in bins of centrality) of dielectrons for Pb + Pb collisions at ($\sqrt{s_{NN}}=5020$ GeV).

the two peripheral samples, and comparable to the cocktail and thermal radiation yields in semi-central collisions. The impact-parameter dependent dilepton P_T distribution is described by a Wigner function generalization of the Weizsäcker-Williams fluxes. Different weights of $J_z = 0, \pm 2$ channels of the $\gamma\gamma$ -system. For e^+e^- pairs the $J_z = \pm 2$ channels dominate. The *parameter free* Wigner function approach gives very good description of centrality dependence of pair transverse momentum and lepton azimuthal decorrelation.

Acknowledgements

Funding information The work reported here was partially supported by the Polish National Science Center (NCN) grant UMO-2018/31/B/ST2/03537.

References

- [1] G. Baur, K. Hencken, D. Trautmann, S. Sadovsky and Y. Kharlov, “Coherent gamma gamma and gamma-A interactions in very peripheral collisions at relativistic ion colliders,” Phys. Rept. **364** (2002), 359-450 [arXiv:hep-ph/0112211 [hep-ph]].
- [2] C. A. Bertulani, S. R. Klein and J. Nystrand, “Physics of ultra-peripheral nuclear collisions,” Ann. Rev. Nucl. Part. Sci. **55** (2005), 271-310 [arXiv:nucl-ex/0502005 [nucl-ex]].
- [3] S. Klein and P. Steinberg, “Photonuclear and Two-photon Interactions at High-Energy Nuclear Colliders,” Ann. Rev. Nucl. Part. Sci. **70** (2020), 323-354 [arXiv:2005.01872 [nucl-ex]].
- [4] N. Baron and G. Baur, “Unraveling gamma gamma dileptons in central relativistic heavy ion collisions,” Z. Phys. C **60** (1993), 95-100
- [5] W. Schäfer, “Photon induced processes: from ultraperipheral to semicentral heavy ion collisions,” Eur. Phys. J. A **56** (2020) no.9, 231
- [6] S. R. Klein and J. Nystrand, “Photoproduction of quarkonium in proton proton and nucleus nucleus collisions,” Phys. Rev. Lett. **92** (2004), 142003 [arXiv:hep-ph/0311164 [hep-ph]].
- [7] V. P. Goncalves and M. V. T. Machado, “The QCD pomeron in ultraperipheral heavy ion collisions. IV. Photonuclear production of vector mesons,” Eur. Phys. J. C **40** (2005), 519-529 [arXiv:hep-ph/0501099 [hep-ph]].
- [8] W. Schäfer and A. Szczurek, Phys. Rev. D **76** (2007), 094014 [arXiv:0705.2887 [hep-ph]].
- [9] B. Z. Kopeliovich and B. G. Zakharov, “Quantum effects and color transparency in charmonium photoproduction on nuclei,” Phys. Rev. D **44** (1991), 3466-3472.
- [10] N. N. Nikolaev, “Quantum mechanics of color transparency,” Comments Nucl. Part. Phys. **21**, no. 1, 41 (1992).
- [11] A. Łuszczak and W. Schäfer, “Incoherent diffractive photoproduction of J/ψ and Υ on heavy nuclei in the color dipole approach,” Phys. Rev. C **97** (2018) no.2, 024903 [arXiv:1712.04502 [hep-ph]].
- [12] A. Łuszczak and W. Schäfer, “Coherent photoproduction of J/ψ in nucleus-nucleus collisions in the color dipole approach,” Phys. Rev. C **99** (2019) no.4, 044905 [arXiv:1901.07989 [hep-ph]].
- [13] A. Łuszczak and W. Schäfer, “Coherent photoproduction of J/ψ in nucleus-nucleus collisions in the color dipole approach- an update,” [arXiv:2108.06788 [hep-ph]].
- [14] A. Łuszczak and H. Kowalski, “Dipole model analysis of high precision HERA data,” Phys. Rev. D **89** (2014) no.7, 074051.
- [15] A. Łuszczak and H. Kowalski, “Dipole model analysis of highest precision HERA data, including very low Q^2 's,” Phys. Rev. D **95** (2017) no.1, 014030.

- [16] B. Abelev *et al.* [ALICE Collaboration], Phys. Lett. B **718**, 1273 (2013) [arXiv:1209.3715 [nucl-ex]].
- [17] E. Abbas *et al.* [ALICE Collaboration], Eur. Phys. J. C **73** (2013) no.11, 2617 [arXiv:1305.1467 [nucl-ex]].
- [18] V. Khachatryan *et al.* [CMS Collaboration], Phys. Lett. B **772**, 489 (2017) [arXiv:1605.06966 [nucl-ex]].
- [19] [LHCb Collaboration], “Study of coherent J/ψ production in lead-lead collisions at $\sqrt{s_{NN}} = 5$ TeV with the LHCb experiment,” LHCb-CONF-2018-003, CERN-LHCb-CONF-2018-003.
- [20] S. Acharya *et al.* [ALICE], Phys. Lett. B **798** (2019), 134926 [arXiv:1904.06272 [nucl-ex]].
- [21] S. Acharya *et al.* [ALICE], [arXiv:2101.04577 [nucl-ex]].
- [22] N. N. Nikolaev and B. G. Zakharov, Z. Phys. C **64**, 631 (1994).
- [23] N. N. Nikolaev, B. G. Zakharov and V. R. Zoller, Phys. Lett. B **328** (1994), 486-494.
- [24] N. N. Nikolaev, W. Schäfer, B. G. Zakharov and V. R. Zoller, JETP Lett. **84**, 537 (2007).
- [25] I. Tserruya, Landolt-Bornstein **23** (2010), 176 [arXiv:0903.0415 [nucl-ex]].
- [26] R. Rapp, Adv. High Energy Phys. **2013** (2013), 148253 [arXiv:1304.2309 [hep-ph]].
- [27] M. Kłusek-Gawenda, R. Rapp, W. Schäfer and A. Szczurek, “Dilepton Radiation in Heavy-Ion Collisions at Small Transverse Momentum,” Phys. Lett. B **790** (2019), 339-344 [arXiv:1809.07049 [nucl-th]].
- [28] R. Rapp and E. V. Shuryak, “Thermal dilepton radiation at intermediate masses at the CERN - SPS,” Phys. Lett. B **473** (2000), 13-19 [arXiv:hep-ph/9909348 [hep-ph]].
- [29] M. Kłusek-Gawenda, W. Schäfer and A. Szczurek, “Centrality dependence of dilepton production via $\gamma\gamma$ processes from Wigner distributions of photons in nuclei,” Phys. Lett. B **814** (2021), 136114 [arXiv:2012.11973 [hep-ph]].
- [30] S. Klein, A. H. Mueller, B. W. Xiao and F. Yuan, “Lepton Pair Production Through Two Photon Process in Heavy Ion Collisions,” Phys. Rev. D **102** (2020) no.9, 094013 [arXiv:2003.02947 [hep-ph]].
- [31] J. D. Brandenburg, W. Zha and Z. Xu, “Mapping the electromagnetic fields of heavy-ion collisions with the Breit-Wheeler process,” Eur. Phys. J. A **57** (2021) no.10, 299 [arXiv:2103.16623 [hep-ph]].
- [32] S. Lehner [ALICE], PoS **LHCP2019** (2019), 164 doi:10.22323/1.350.0164 [arXiv:1909.02508 [nucl-ex]].
- [33] [ATLAS], “Measurement of non-exclusive dimuon pairs produced via $\gamma\gamma$ scattering in Pb+Pb collisions at $\sqrt{s_{NN}} = 5.02$ TeV with the ATLAS detector,” ATLAS-CONF-2019-051.